Metformin confers sensitisation to syrosingopine in multiple myeloma cells by metabolic blockage and inhibition of protein synthesis

Van der Vreken, Arne; Oudaert, Inge; Ates, Gamze; Faict, Sylvia; Vlummens, Philip; Satilmis, Hatice; Fan, Rong; Maes, Anke; Massie, Ann; De Veirman, Kim; De Bruyne, Elke; Vanderkerken, Karin; Menu, Eline

Published in:
Journal of pathology

DOI:
10.1002/path.6066

Publication date:
2023

License:
Unspecified

Document Version:
Accepted author manuscript

Metformin confers sensitization to syrosingopine in Multiple Myeloma cells by metabolic blockage and inhibition of protein synthesis

Arne Van der Vreken[1]†, Inge Oudaert[1]†, Gamze Ates[2], Sylvia Faict[3], Philip Vlummens[1,4], Hatice Satilmis[1], Rong Fan[1], Anke Maes[1], Ann Massie[2], Kim De Veirman[1], Elke De Bruyne[1], Karin Vanderkerken[1], Eline Menu[1]*

[1]Department of Hematology and Immunology, Myeloma Center Brussels, Vrije Universiteit Brussel, Brussels (VUB), Belgium.

[2]Center for Neurosciences, Neuro-Aging & Viro-Immunotherapy, Vrije Universiteit Brussel, Brussels, Belgium

[3]Department of Hematology, Vrije Universiteit Brussel, Universitair Ziekenhuis Brussel, Brussels, Belgium

[4]Department of Clinical Hematology, Ghent University Hospital, Ghent, Belgium

† Equal contributions

Short running title: Combination of syrosingopine and metformin to treat multiple myeloma

Word count: 3991

***Correspondence to:** E Menu, , Department of Hematology and Immunology , Vrije Universiteit Brussel, Laarbeeklaan 103, 1090 Brussels, Belgium. E-mail: Eline.Menu@vub.be

ORCID: 0000-0002-0805-6581

Declaration of competing interest: The authors declare no conflict of interest.

Abstract

Multiple myeloma (MM) remains an incurable haematological malignancy despite substantial advances in therapy. The hypoxic bone marrow induces metabolic rewiring in MM cells contributing to survival and drug resistance. Therefore, targeting metabolic pathways may offer an alternative treatment option. In this study, we re-purpose two FDA-approved drugs, syrosingopine and metformin. Syrosingopine was used as a dual inhibitor of monocarboxylate transporter 1 and 4 (MCT1/4) and metformin as an inhibitor for oxidative phosphorylation (OXPHOS). Anti-tumour effects were evaluated for single agents and in combination therapy. Survival and expression data for MCT1/MCT4 were obtained from the TT2, Mulligan and MMRF-cohort. Cell death, viability and proliferation were measured using Annexin V/7-AAD, CellTiterGlo and BrdU, respectively. Metabolic effects were assessed using Seahorse Glycolytic Rate assays and LactateGlo assays. Differential protein expression was determined using western blotting and the SUnSET method was implemented to quantify protein synthesis. Finally, the syngeneic 5T33MMvv model was used for *in vivo* analysis. High level expression of MCT1 and MCT4 both correlated with a significantly lower overall survival of patients. Lactate production as well as MCT1/MCT4 expression were significantly upregulated in hypoxia, confirming the Warburg effect in MM. Dual inhibition of MCT1/4 with syrosingopine resulted in intracellular lactate accumulation and reduced cell viability and proliferation. However, only at higher doses (>10 μM), was syrosingopine able to induce cell death. By contrast, combination treatment of syrosingopine with metformin was highly cytotoxic for MM cell lines and primary patient samples and resulted in a suppression of both glycolysis and OXPHOS. Moreover, pathway analysis revealed an upregulation of the energy sensor p-AMPKα, and more downstream a reduction in protein synthesis. Finally, the combination treatment resulted in a significant reduction in tumour burden *in vivo*. This study proposes an alternative combination treatment for MM and provides insight in the intracellular effects.

Keywords: Multiple myeloma, monocarboxylate transporters, lactate metabolism, protein synthesis, syrosingopine, metformin

Introduction

Multiple myeloma (MM) is a haematological malignancy originating from malignant plasma cells, which have engrafted and accumulate in the bone marrow (BM) [1]. Despite substantial advances in therapeutic strategies, the disease remains incurable. Emergence of drug-resistant cells can be partly attributed to their development and survival in the hypoxic BM environment that forms a protective niche. This hypoxia favours metabolic rewiring of the MM cells, characteristic of a more resistant phenotype [2–5].

Malignant cells display a metabolic plasticity and can switch from oxidative phosphorylation (OXPHOS) to the less efficient aerobic glycolysis for rapid ATP production [5]. Cancer cells increase their glycolytic rate to compensate, resulting in an increased conversion of pyruvate to lactate. This phenomenon is also known as the Warburg effect, which is well described for several solid cancers such as colorectal cancer and non-small cell lung carcinoma [6,7]. However, its role in MM is less defined.

To cope with accumulation of lactate and acidification, cells export lactate via monocarboxylate transporters (MCTs) [8]. MCTs shuttle monocarboxylates such as L-lactate across the cell membrane in a proton-linked manner. Several MCT isoforms have been described, however only four can transport lactate (MCT1–4). MCT1 is a bidirectional transporter ubiquitously expressed among tissues, whereas MCT2 is expressed in testicular tissue, brain, and renal tubules. MCT3 is only expressed in retinal tissue and choroid plexus [8]. MCT4 is upregulated in hypoxia via hypoxia-inducible factor 1α (HIF1α) and allows glycolytic cells to rapidly export lactate out of the cell [9]. Overexpression of MCTs in glycolyzing tumour cells allows them to export lactate that would otherwise become toxic. MCTs may therefore be a particularly important target in glycolyzing tumours or tumours growing in a hypoxic environment such as the BM [9]. Several studies reported that the overexpression of MCT1 and MCT4 in malignant cells maintains cellular homeostasis and their expression on tumour cells is associated with a poor prognosis in the case of solid

tumours [10–12]. For MM, it has also been described that MCT1 is a marker for therapy resistance [13]. Inhibition of MCTs leads to intracellular lactate accumulation and decreased the cellular pH, resulting in a reduced cell proliferation in both solid and haematological cancers [14–16]. One MCT1 inhibitor, AZD3965, is currently in clinical trial (phase 1) for patients with advanced Burkitt's lymphoma and diffuse large B-cell lymphoma (NCT01791595). However, cells with high MCT4-expression showed resistance to AZD3965 [17]. Therefore, simultaneous inhibition of MCT1 and MCT4 might be a more feasible strategy. Recently, syrosingopine (FDA-approved anti-hypertensive drug) was described as dual inhibitor of MCT1 and MCT4, showing good potency for both transporters [18]. Moreover, it has been shown that the hampered proliferation caused by MCT inhibition can be augmented with anti-diabetic biguanides such as metformin and phenformin [19]. These drugs cause specific inhibition of complex I (NADH: ubiquinone oxidoreductase) of the electron transport chain, preventing the oxidation of NADH to NAD^+ leading to decreased ATP levels [20]. MCT inhibition generates an intracellular accumulation of lactate, resulting in negative feedback on lactate dehydrogenase, which effectuates the conversion of pyruvate to lactate. Simultaneously with this conversion, co-factor NADH is oxidized to NAD^+. Mechanistically, the combination of syrosingopine and metformin results in a NAD^+ depletion, leading to a block in glycolysis [18]. However, the intracellular effects of this dual inhibition on cancer cells needs to be further elucidated.

The present study shows that metformin in combination with dual inhibition of MCT1 and MCT4 by syrosingopine not only results in a potent cytotoxic activity against MM cell lines and primary MM cells, but also has anti-tumour activity *in vivo*. We found that these FDA-approved drugs cause inhibition of glycolysis and OXPHOS, leading to decreased energy levels. Mechanistically, the phosphorylation of the energy sensor AMPKα was enhanced, leading to downstream inhibition of the mTOR-pathway and a reduction in protein synthesis. Taken together, we demonstrate that the syrosingopine/ metformin combination has significant therapeutic potential in MM.

Materials and methods

Gene expression data

Gene expression profiling data of the total therapy 2 (TT2) cohort [21,22] and Mulligan cohort [23] were consulted via the web tool Genomicscape (http://www.genomicscape.com). The TT2 cohort is a microarray-based gene expression data set of 345 newly diagnosed MM patients from the University of Arkansas for Medical Sciences (UAMS, AR, USA; GSE2658), while the Mulligan cohort contains microarray-based gene expression data set of 264 MM patients (GSE9782). Data were analysed using the MAS5 algorithm [24]. The MMRF CoMMpass Trial (NCT01454297) [25] comprises DNA- and RNA-seq data obtained at diagnosis and at subsequent relapse. Data from this longitudinal study are publicly available (research.themmrf.org). Survival curves were plotted using data from 653 patients, while expression levels comparing newly diagnosed to matched relapsed/refractory samples were available for 49 patients.

Cell culture

Human myeloma cell lines (HMCLs) OPM-2, LP-1, RPMI-8226, JJN-3 and ANBL-6 (ATCC, Molsheim, France) were cultured in RPMI-1640 medium (Thermo Fisher Scientific, Aalst, Belgium), supplemented with 10% heat-inactivated fetal bovine serum (Hycone, Logan, UT, USA), 2 mM L-glutamine, and 100 Units/ml penicillin/streptomycin (Thermo Fisher Scientific) at 37 °C in 5% CO_2. The BM stromal cell line HS-5 (ATCC) was cultured in DMEM medium (Thermo Fisher Scientific), supplemented with 10% heat-inactivated fetal bovine serum. Short-tandem repeat analysis was performed on a regular basis to confirm cell line identity.

Hypoxic culture conditions

All experiments were performed in hypoxia, unless indicated otherwise. HMCL were incubated in a hypoxia chamber (STEMCELL™ technologies, Grenoble, France) filled with a gas mixture of 1% O_2, 5% CO_2 and 94% N_2. RPMI-1640 medium was supplemented with 2 mM HEPES buffer (Thermo Fisher Scientific).

Tracer study

RPMI-8226 cells were cultured for 48 h in normoxia (21 % O_2) and hypoxia (1 % O_2) in RPMI-1640 medium, supplemented with 10 mM ^{13}C-glucose. Supernatant was isolated and shipped on dry ice to Metabolomics Expertise Center (MEC; VIB-KU Leuven, Belgium) for further analysis. Data were normalized to cell numbers.

Compounds

Syrosingopine and metformin were both purchased from Sigma Aldrich (Merckx Life Science, Hoeilaart, Belgium) and AZD3965 from Selleckchem (Munich, Germany). DZD0095 was kindly provided by Dizal Pharma (Shanghai, PR China). Syrosingopine, AZD3965 and DZD0095 were all dissolved in dimethylsulphoxide (DMSO) at a stock concentration of 15 mM. Metformin was dissolved in PBS (Gibco) at a stock concentration of 1.87 M.

Reverse Transcription- quantitative PCR (RT-qPCR)

RNA was isolated by the NucleoSpin® RNA Plus kit (Macherey-Nagel, Filter Service S.A., Eupen, Belgium) according to the manufacturer's instructions. A total of 1 µg RNA was used for cDNA synthesis using a cDNA synthesis kit (Thermo Fisher Scientific). The reactions were performed in a SWIFT MiniPro Thermal Cycler (Esco LifeSciences, Germany). Quantitative real-time PCR (was performed using the SYBR Green dye (Applied Biosystems, Thermo Fisher Scientific). The mRNA expression levels were quantified using the QuantStudio 12K Flex Real-Time PCR System (Thermo Fisher Scientific) and normalized to the reference transcript *ACTB*. Primer sequences (IDT, Leuven, Belgium): SLC16A1 forward (5'-CATTGGCATGGGCATCAATTATC-3') and reverse (5'-GGCTTCCCAGCAACATCTATAC-3'), SLC16A3 forward (5'-TCTTCGGCTGTTTCGTCATC-3') and reverse (5'-CCGATCCCAAACTCCTGTATG-3').

Cell viability and apoptosis assays

Cells were seeded at 500,000 cells/ml. Viability was determined using the CellTiter-Glo® Luminescent cell viability assay (Promega, Madison, WI, USA) and apoptosis was quantified using Annexin V-APC/7-AAD (BD Biosciences, Erembodegem, Belgium). Samples were analysed using a FACSCanto flowcytometer (BD Biosciences).

Lactate levels

50,000 cells were incubated in 100 µl of RPMI-1640 for 3 h in hypoxia. Intracellular lactate accumulation was determined using the Lactate-Glo® Assay (Promega).

Western blotting

Cells were lysed and blotted as previously described [2,26]. We used following antibodies: p-AMPKα (##2535), AMPKα (##5831), p-mTOR (#5536), mTOR (#2983), p-P70S6K (#9234), P70S6K (#2708), p-S6 (#4858), S6 (#2217), p-4EBP1 (#2855), 4EBP1 (#9644), p-eIF4E (#9741), eIF4E (#2067), β-ACTIN (#4967), α-TUBULIN (#2144), horseradish peroxidase-coupled anti-rabbit (#7074) and anti-mouse (#7076), all purchased from Cell Signaling Technology (Leiden, The Netherlands). MCT1 (SC365501) and MCT4 (SC376140) were purchased from Santa Cruz Biotechnology (Heidelberg, Germany). Chemiluminescence was visualized using the LI-COR Odyssey Fc platform (LI-COR, Bad Homburg, Germany). Pixel intensities were determined using ImageJ software (v1.53, https://imagej.nih.gov/ij/, last accessed on 10/06/2022) or Image Studio Lite (v5.2, https://licor.app.box.com/s/4hrk823vov7vittqjg3onj51tb0wbo6w, last accessed on 05/09/2022).

Puromycin uptake

Global protein synthesis was determined using the SUnSET method [27]. Cells were treated with 1 µM of puromycin (Cat. Nr. S7417, Selleckchem) 30 min before pellet isolation. Pellets

were used for western blotting. To detect puromycin uptake, we used an anti-puromycin antibody (#MABE343, Sigma-Aldrich, Diegem, Belgium).

Metabolic analyses

After 16 h of treatment, cells were washed twice with Seahorse RPMI assay medium (supplemented with 2 mM glutamine, 1 mM pyruvate and 10 mM glucose) and seeded at 50,000 cells/well in XFe96-well plates (Agilent Technologies, Belgium) that had been precoated with Cell-Tak (Corning, Louvain-La-Neuve, Belgium) one day prior to the assay and stored at 4 °C. The glycolytic rate assay was performed following the manufacturer's instructions. After real-time measurement of OCR and ECAR, cells were stained with Hoechst 33342 (16 µM, 30 min incubation in the dark, Sigma-Aldrich) and cells counted automatically using a Cytation1 cell imaging multimode reader (BioTek instruments). Data were normalized to cell number.

Cell proliferation assays

Cells were treated for 20 h, followed by incubation with bromodeoxyuridine (BrdU; 1 mg/ml) for 4 h. Cells were then fixed with paraformaldehyde for 10 min at 4 °C and stored overnight in PBS containing 0.2 % Tween (Sigma-Aldrich) at room temperature. Cells were washed, permeabilized with 250 µl 2 M HCl and stained using anti-BrdU-fluorescein conjugate (#1120269001, Sigma-Aldrich). Cells were analysed using a FACSCanto flow cytometer.

Primary myeloma samples

BM samples from patients were obtained from UZ Brussel with the patient's informed consent, conforming to the declaration of Helsinki and with approval of the institutional research board (B.U.N. 143201838414). Peripheral blood mononuclear cells were isolated using Lymphoprep™ (STEMCELL™ technologies, Grenoble, France) and labelled with CD138-Microbeads (Miltenyi Biotec, Gladbach, Germany). The CD138-positive fraction was isolated by magnetic activated cell sorting.

Syngeneic 5T33MMvv mice and treatment

C57BL/KalwRij mice were purchased from Envigo Laboratories (Horst, The Netherlands). Housing, follow-up and treatment conditions were approved by the Ethical Committee for Animal Experiments of the Vrije Universiteit Brussel (License No LA1230281, CEP No 20-281-6). Mice were transplanted with 0.50 million cells from diseased BM and treated intraperitoneally with 7.5 milligram/kilogram (mpk) syrosingopine (in 66 % DMSO, 34 % PBS) and 200 mpk metformin (in PBS), 3 times a week. After 18 days, vehicle-treated mice showed signs of paralysis and all mice were sacrificed. Total BM was collected and intracellularly stained with an *in house* purified 3H2 anti-idiotype antibody. Cells were analysed using flow cytometry.

Statistical analyses

Statistical analyses were performed using Prism 9 software (GraphPad Inc, San Diego, CA, USA). Data are presented as mean ± SD, and either the Mann–Whitney-U or Kruskal–Wallis test or the one-way ANOVA test was used. $p \leq 0.05$ (*), $p \leq 0.01$ (**), $p \leq 0.001$ (***) and $p \leq 0.0001$ (****) were used to indicate significance. Synergy scores were calculated using the Chou–Talalay method.

Results

High expression levels of MCT1 and MCT4 in malignant plasma cells are correlated with poor survival in Multiple Myeloma

To evaluate the clinical relevance of MCT1 and MCT4 in MM, we consulted the publicly available gene expression profiling data of several MM patient cohorts. Analysis of the Mulligan cohort [23] revealed that high expression levels of *SLC16A1* (MCT1) ($p = 0.0015$) and of *SLC16A3* (MCT4) ($p = 0.0079$) correlated with significantly lower overall survival of MM patients (Figure 1A). Similar associations were observed in the MMRF cohort [25] (supplementary material, Figure S1A). Gene expression data from the Total therapy (TT2) cohort [21,22] were used to compare MCT mRNA expression in plasma cells from healthy

individuals with those in different stages of MM progression (Figure 1B). Compared to high levels of *SLC16A1* (MCT1) expression in plasma cell samples of MM patients (n=345), lower levels were observed in samples from healthy people (n=22), from patients with monoclonal gammopathy of undetermined clinical significance (MGUS) (n=44) and smouldering multiple myeloma (SMM) (n=12). *SLC16A3* (MCT4) was only increased in some MM patients. However, in the MMRF cohort [25] *SLC16A3* (MCT4) expression was significantly increased in samples from relapsed MM patients compared to their matched-newly diagnosed samples (supplementary material, Figure S1B). The protein expression of MCT1 and MCT4 was further validated in primary BM derived $CD138^+$ cells by western blotting (Figure 1C), where MCT1 was detectable in three out of four samples, while only two samples showed low MCT4 expression.

Lactate production and export are both upregulated in hypoxic MM cells

Basal expression levels of MCT1 and MCT4 in HMCL were measured at mRNA and protein level, using RT-qPCR and western blotting, respectively. Several HMCL originating from distinct MM subclasses were tested (MMSET: OPM-2, MMSET/FGFR3: LP-1, cMAF: RPMI-8226 and JJN-3, IL-6 dependent cell line ANBL-6) (Figure 2A,B) [28]. A heterogeneous MCT4 expression was noted, with the highest levels in RPMI-8226 cells. MCT1 was more uniformly expressed across the tested cell lines, with the lowest level in OPM-2. Based on their differential MCT4 expression, RPMI-8226 and LP-1 cells were selected for further *in vitro* experiments. MCT1 and MCT4 expression levels of these lines were tested when cultured in normoxic (21% O_2) and hypoxic (1% O_2) conditions (Figure 2C,D). For MCT1, a significant upregulation was observed in both LP-1 and RPMI-8226 cells, while MCT4 was significantly upregulated in RPMI-8226 cells. Next, a tracer study was performed in RPMI-8226 cells to evaluate ^{13}C-glucose-to-lactate conversion. Conversion was indeed significantly increased under hypoxic conditions (Figure 2E). Our data indicate that MM cells faced with hypoxia rely more on glycolysis for their ATP generation and adapt by upregulating lactate exporters.

Inhibition of MCT1 and MCT4 with syrosingopine reduces proliferation of MM cells.

Under hypoxic conditions, the RPMI-8226 cells increase their reliance on glycolysis and are more dependent on lactate efflux. Therefore, they would be more sensitive to inhibitors of lactate efflux, such as syrosingopine. Here, we tested syrosingopine under low-oxygen conditions (1%), mimicking the hypoxic BM.

First, the ability of syrosingopine to inhibit both MCT1 and MCT4 was assessed (Figure 3A). LP-1 and RPMI-8226 were treated with either DMSO or increasing concentrations (1-15 μM) of syrosingopine. A dose-dependent intracellular increase in lactate was observed after 3 h incubation. Next, the anti-tumour effects were evaluated. A decreased relative viability was observed for LP-1 cells starting from 5 μM, and for RPMI-8226 starting from 10 μM after 48 h of incubation (Figure 3B). Significant increases of apoptotic and necrotic RPMI-8226 and LP-1 cells occurred at 10 μM syrosingopine (Figure 3C). BrdU incorporation was decreased in a dose-dependent manner for both cell lines, suggesting a reduction in cell proliferation (Figure 3D). These data imply that syrosingopine targets lactate secretion, with an impact on cell viability.

Combination treatment of syrosingopine and metformin is cytotoxic for MM cells

To test whether addition of the antidiabetic compound metformin can augment the activity of syrosingopine, HMCLs and primary MM cells from patient samples were treated with a low dose of metformin (10 mM) and the effective dose of syrosingopine (10 μM). Both RPMI-8226 and LP-1 cells were cultured in hypoxia for 48 h and 72 h, respectively. For both HMCLs the combination treatment resulted in a significantly reduced relative viability when compared to treatment with the single agents or DMSO (Figure 4A). No reduction in cell viability was observed for stromal HS-5 cells (supplementary material, Figure S2A). To determine whether dual MCT1/4 inhibition is necessary for metformin to sensitize cells to syrosingopine, we used two inhibitors which were either specific for MCT1 (AZD3965) or MCT4 (DZD0095). Neither the combination with metformin and AZD3965 or DZD0095 resulted in a decreased cell

viability of the RPMI-8226 cells (supplementary material, Figure S2B). However, combining AZD3965 and DZD0095 with metformin resulted in a significant reduction in MM cell viability (supplementary material, Figure S2C). Next, freshly isolated CD138+ cells from six patient samples were treated with the combination treatment and evaluated for effects on cell viability (Figure 4B). Metformin significantly potentiated the effect of syrosingopine in these samples. Additionally, both HMCLs showed a significant increase in cell death compared to the single agents and DMSO treated cells (Figure 4C). To determine whether their effect was synergistic, the two HMCLs were treated with three different concentrations of each drug and analysed using the Chou–Talalay method. This demonstrated that the proposed combination was indeed highly synergistic (supplementary material, Figure S2D). Finally, the combination treatment was evaluated in the syngeneic 5T33MMvv mouse model (Figure 4D). M-spike levels in the blood of diseased mice was used as general indicator for MM. While syrosingopine as single agent already lowered M-spike levels in the serum (average 3.7 g/dl), only the combination strategy resulted in a significant reduction, compared to vehicle treated mice (average 1.9 g/dl compared to 4.9 g/dl) (Figure 4E). Analysis of 3H2 idiotype expression, as a measure to identify MM cells in the BM, showed a non-significant reduction of 3H2pos 5T33MM cells in the BM of both syrosingopine (19%) and combination treated mice (16% versus 25% in vehicle) (Figure 4F). By contrast, effects on MM-induced splenomegaly, were more pronounced. We found the most significant effects in the combination group (0.13 g versus 0.18 g for syrosingopine and 0.3 g for vehicle), suggesting that higher concentrations of the drugs could be reached in the spleen compared to the BM (Figure 4G). All together, these data demonstrate that metformin synergizes with syrosingopine resulting in reduced cell viability in vitro and tumour burden *in vivo*.

Metformin and syrosingopine causes metabolic blockage in MM cells

To evaluate the metabolic status of MM cells treated with these compounds, the oxygen consumption rate (OCR) and extracellular acidification rate (ECAR) were determined as

measures for OXPHOS and glycolysis, respectively. The proton efflux rate (PER) comprises acidification of OXPHOS and glycolysis. Rotenone/ antimycin A (Rot/AA, 0.5 μM) was used as inhibitor of OXPHOS and 2-deoxyglucose (2-DG, 50 mM) as inhibitor of glycolysis. Cells were stained with Hoechst to exclude the metabolism of dead cells. Figure 5A shows that metformin inhibited OXPHOS in both LP-1 and RPMI-8226 cells. Metformin-treated cells showed a more elevated ECAR and PER, indicating an increased compensatory glycolytic rate (Figure 5B,C). By contrast, treatment with syrosingopine resulted in lowered ECAR and PER, consistent with a diminished glycolytic rate. These data demonstrate that combined treatment of MM cells with syrosingopine and metformin successfully inhibits two crucial metabolic pathways, namely glycolysis and OXPHOS.

Combination treatment of syrosingopine and metformin results in increased p-AMPKα and reduced protein synthesis

Combined shut-off of glycolysis and OXPHOS by syrosingopine/metformin treatment may activate the AMPK pathway leading to mTOR inhibition. In order to investigate whether this feedback response takes place, we treated MM cells with 10 μM syrosingopine and 10 mM metformin and placed in hypoxia for 16 h (Figure 6A,B). In RPMI-8226 cells the p-AMPKα levels were significantly higher following the combination treatment compared to treatment with syrosingopine only or DMSO (supplementary material, Figure S3A,B). In LP-1 cells a small but non-significant increase was seen. However, p-mTOR levels in the combination group were significantly reduced when compared to the other treatments.

The next series of experiments focused on the proteins more downstream of mTOR, and on the phosphorylation status of proteins involved in the protein synthesis pathway: S6, P70S6K and 4EBP1. Western blotting and pixel intensity analysis revealed a significant decrease in phosphorylation levels of p-S6, p-P70S6K and p-4EBP1 for RPMI-8226 cells exposed to the syrosingopine/metformin combination. In LP-1 cells p-S6 was reduced (Figure 6A,B, supplementary material, Figure S4A,B). Other phospho-proteins in the protein synthesis

pathway were also, but non-significantly, reduced in this group. Treatment with the single agents did not affect any of the investigated proteins. These data indicate that the combined treatment with syrosingopine and metformin results in a reduced protein synthesis upon metabolic blockage, which might be regulated via p-AMPKα. To further validate protein synthesis inhibition, the SUnSET method was used (Figure 6B). This method is based on the incorporation of puromycin in elongating peptides. Detected puromycin by western blotting directly correlates with translation activity. Pixel intensity analysis of five independent experiments revealed a significant decrease of puromycin uptake in the combination group, compared to both single agents and DMSO treated cells (supplementary material, Figure S4C).

Discussion

In this study, we first evaluated the potential of MCT1 and MCT4 as prognostic marker for MM, using the Mulligan and MMRF cohorts. MM cells reside in the hypoxic BM environment, which triggers an increase in aerobic glycolysis, leading to enhanced MCT levels. Our study identified increased expression levels of *SLC16A1* and *SLC16A3* as marker for poor prognosis. This is in analogy with the earlier identification of MCT1 as predictive marker for lenalidomide response in MM [13]. We confirmed MCT1 and MCT4 expression on primary patient samples. Moreover, we are the first to show that MCT protein expression in HMCLs is upregulated under hypoxia.

Next, *in vitro* studies were performed aiming at targeting both MCTs in hypoxia. Inhibition of both transporters with syrosingopine resulted in impaired viability of myeloma cells, while targeting only MCT1 with AZD3965 or MCT4 with DZD0095 had no effect on cell viability. This finding is in accordance with other studies on solid tumour cells, where it has been described that MCT1 can take over the function of MCT4 as a lactate exporter when MCT4 is absent, illustrating the functional redundancy between these two transporters [14,15,29]. However, MCT inhibition alone was insufficient to induce pronounced lethality, therefore the

possibility that a combination with metformin would be more potent was tested. The combination strategy tested in the present study showed enhanced effects when compared to MCT inhibition alone. This is in agreement with the observations of Granja, *et al* [19] and by extension Benjamin, *et al* [18]. Here, we showed for the first time that the combination of syrosingopine and metformin is cytotoxic for 2 HMCLs, patient-derived myeloma cells and significantly reduces the M-protein in MM bearing mice.

Syrosingopine is an FDA-approved drug, already administered as an anti-hypertensive agent. Metformin is an anti-diabetic drug, which is routinely administered in clinic. Epidemiological studies have demonstrated that its use in diabetic patients with MGUS is associated with a reduced risk of progression to MM [30]. Furthermore, its anti-tumour effects in patients are currently being investigated in several clinical trials involving both solid and haematological cancers (https://clinicaltrials.gov/ct2/show/NCT02978547, https://clinicaltrials.gov/ct2/show/NCT04758000, https://clinicaltrials.gov/ct2/show/NCT03118128, last accessed on 01/09/2022). Repurposing approved drugs could be a safe way to target tumour cell metabolism.

Since cancer cells display a high metabolic plasticity, it is important for anti-cancer strategies to ensure that drugs not only efficiently target their main metabolic pathway but also that compensatory pathways are blocked [31,32]. Glycolytic and OXPHOS-related genes are both upregulated in MM, when compared to MGUS, and this upregulation is associated with a more aggressive disease [33]. The study of Benjamin, *et al.* demonstrated that the combination of syrosingopine and metformin lowers the NAD^+ levels, required to drive glycolysis [18]. Here we show for the first time that syrosingopine as single agent already blocks glycolysis in MM cells exposed to hypoxia. Combination treatment is necessary to inhibit both glycolysis and OXPHOS, which is highly cytotoxic for MM cells (Figure 6C).

To determine what could be the link between metabolic inhibition and a block in proliferation and survival, we focused on the cellular energy sensor p-AMPKα, which has been shown to be upregulated upon an elevated AMP/ATP ratio [34]. This was considered particularly relevant since the combination treatment directly lowered the energy status. We could demonstrate for the first time that the combination therapy in hypoxia caused elevated p-AMPKα levels, associated with downstream effects on the protein synthesis pathway. The upregulation of p-AMPKα upon energy starvation and its link to reduced protein synthesis has already been described in MM and solid tumours [34,35]. Pathway investigation showed a decreased phosphorylation status of mTOR, 4EBP1, eIF4E, P70S6K and S6. We and others have shown in MM that a decreased phosphorylation status of mTOR, P70, S6 and 4EBP1 impedes MM progression and induces cell death [36,37]. Moreover, we previously described a link between metabolism and protein synthesis in myeloma, since knock-down of pyrroline-5-carboxylate reductase 1 (PYCR1) reduced protein synthesis and increased sensitivity to the proteasome inhibitor bortezomib [2].

In conclusion, the present study provides novel evidence for the syrosingopine/metformin combination to have potential as an effective treatment for MM. Given the high relapse rate and frequent development of drug resistance in MM, repurposing syrosingopine and metformin could offer a safe and affordable complementary treatment option.

Acknowledgements

The authors thank Charlotte Van De Walle, Carine Seynaeve and Lauren Van Droogenbroeck for their laboratory assistance. This study was supported by the VUB (SRP-48), Kom op tegen kanker, FWO Vlaanderen (medium-scale research infrastructure program; I001420N), VUB-OZR and Fonds Willy Gepts (UZ Brussel). I.O. is pre-doctoral fellow of FWO Vlaanderen (1159622N). K.D.V. is a post-doctoral fellow of FWO Vlaanderen (12I0921N).

Author contributions statement

AVdV, IO and EM designed this study. AVdV, IO, PV, HS an GA collected and interpreted the data. The study was supervised by EM. The manuscript was written by AVdV, IO and EM. All authors read and approved the final manuscript.

Data availability statement

The data that support the findings of this study are available from the corresponding author, EM, upon request.

References

1. Silva AS, Gatenby RA. Adaptation to survival in germinal center is the initial step in onset of indolent stage of multiple myeloma. Mol Pharm. 2011;8(6):2012–20.
2. Oudaert I, Satilmis H, Vlummens P, De Brouwer W, Maes A, Hose D, et al. Pyrroline-5-Carboxylate Reductase 1: a novel target for sensitizing multiple myeloma cells to bortezomib by inhibition of PRAS40-mediated protein synthesis. J Exp Clin Cancer Res . 2022;41: 45.
3. Oudaert I, Van der Vreken A, Maes A, De Bruyne E, De Veirman K, Vanderkerken K, et al. Metabolic cross-talk within the bone marrow milieu: focus on multiple myeloma. Exp Hematol Oncol. 2022;11: 49.
4. Suzuki K, Nishiwaki K, Yano S. Treatment strategies considering micro-environment and clonal evolution in multiple myeloma. Cancers (Basel). 2021;13:‑ 215.
5. Potter M, Newport E, Morten KJ. The Warburg effect: 80 years on. Biochem Soc Trans. 2016;44(5):1499–505.
6. Natarajan SR, Ponnusamy L, Manoharan R. MARK2/4 promotes Warburg effect and cell growth in non-small cell lung carcinoma through the AMPKα1/mTOR/HIF-1α signaling pathway. Biochim Biophys Acta - Mol Cell Res . 2022;1869(7):119242.
7. Meng F, Luo X, Li C, Wang G. LncRNA LINC00525 activates HIF-1α through miR-338-3p / UBE2Q1 / β-catenin axis to regulate the Warburg effect in colorectal cancer. Bioengineered. 2022;13(2):2554–67.
8. Halestrap AP. The SLC16 gene family-Structure, role and regulation in health and disease. Mol Aspects Med. 2013;34(2–3):337–49.
9. Ullah MS, Davies AJ, Halestrap AP. The plasma membrane lactate transporter MCT4, but not MCT1, is up-regulated by hypoxia through a HIF-1α-dependent mechanism. J Biol Chem 2006;281(14):9030–7.
10. Bovenzi CD, Hamilton J, Tassone P, Johnson J, Cognetti DM, Luginbuhl A, et al. Prognostic Indications of Elevated MCT4 and CD147 across Cancer Types: A Meta-

Analysis. Biomed Res Int. 2015; 2015: 242437.

11. Yuan C, Zhang J, Lou J, Wang S, Jiang Y, Wu F, et al. Comprehensive Analysis of Monocarboxylate Transporter 4 (MCT4) expression in breast cancer prognosis and immune infiltration via integrated bioinformatics analysis. Bioengineered. 2021;12(1):3850–63.
12. de Carvalho PA, Bonatelli M, Cordeiro MD, Coelho RF, Reis S, Srougi M, et al. MCT1 expression is independently related to shorter cancer-specific survival in clear cell renal cell carcinoma. Carcinogenesis. 2021;42(12):1420–7.
13. Stroh J, Seckinger A, Heider M, Rudelius M, Eichner R, Schick M, et al. MCT1 is a predictive marker for lenalidomide maintenance therapy in multiple myeloma. Blood Adv. 2022;6(2):515–20.
14. Zhao Z, Wu M si, Zou C, Tang Q, Lu J, Liu D, et al. Downregulation of MCT1 inhibits tumor growth, metastasis and enhances chemotherapeutic efficacy in osteosarcoma through regulation of the NF-κB pathway. Cancer Lett. 2014;342(1):150–8.
15. Saulle E, Spinello I, Quaranta MT, Pasquini L, Pelosi E, Iorio E, et al. Targeting Lactate Metabolism by Inhibiting MCT1 or MCT4 Impairs Leukemic Cell Proliferation, Induces Two Different Related Death-Pathways and Increases Chemotherapeutic Sensitivity of Acute Myeloid Leukemia Cells. Front Oncol. 2021;10: 621458.
16. Hanson DJ, Nakamura S, Amachi R, Hiasa M, Oda A, Tsuji D, et al. Oncotarget 33568 www.impactjournals.com/oncotarget Effective impairment of myeloma cells and their progenitors by blockade of monocarboxylate transportation. Oncotarget 2015;6(32).
17. Blackhall F. Activity of the monocarboxylate transporter 1 inhibitor AZD3965 in small cell lung cancer. Ann Oncol. 2015;26(4):ii15.
18. Benjamin D, Robay D, Hindupur SK, Pohlmann J, Colombi M, El-Shemerly MY, et al. Dual Inhibition of the Lactate Transporters MCT1 and MCT4 Is Synthetic Lethal with Metformin due to NAD+ Depletion in Cancer Cells. Cell Rep 2018;25(11):3047-3058.e4.
19. Granja S, Marchiq I, Le Floch R, Moura CS, Baltazar F, Pouysségur J. Disruption of

BASIGIN decreases lactic acid export and sensitizes non-small cell lung cancer to biguanides independently of the LKB1 status. Oncotarget. 2015;6(9):6708–21.

20. Foretz M, Guigas B, Bertrand L, Pollak M, Viollet B. Metformin: From mechanisms of action to therapies. Cell Metab. 2014;20(6):953–66

21. Zhan F, Barlogie B, Arzoumanian V, Huang Y et al. Gene-expression signature of benign monoclonal gammopathy evident in multiple myeloma is linked to good prognosis. Blood 2007 Feb 15;109(4):1692-700. PMID: 17023574

22. Driscoll JJ, Pelluru D, Lefkimmiatis K, Fulciniti M et al. The sumoylation pathway is dysregulated in multiple myeloma and is associated with adverse patient outcome. Blood 2010 Apr 8;115(14):2827-34. PMID: 19965618

23. Mulligan G, Mitsiades C, Bryant B, Zhan F et al. Gene expression profiling and correlation with outcome in clinical trials of the proteasome inhibitor bortezomib. Blood 2007 Apr 15;109(8):3177-88.

24. Affymetrix Inc. Guide to probe logarithmic intensity error (PLIER) estimation, *Technical note*, 2005, Santa Clara, CA, USA.

25. Keats JJ, Craig DW, Liang W, Venkata Y, Kurdoglu A, Aldrich J, Auclair D, Allen K, Harrison B, Jewell S, Kidd PG, Correll M, Jagannath S, Siegel DS, Vij R, Orloff G, Zimmerman TM, MMRF CoMMpass Network, Capone W, Carpten J, Lonial S. Interim Analysis Of The MMRF CoMMpass Trial, a Longitudinal Study In Multiple Myeloma Relating Clinical Outcomes To Genomic and Immunophenotypic Profiles Blood 2013; 122:532

26. De Bruyne E, Bos TJ, Schuit F, Van Valckenborgh E, Menu E, Thorrez L, et al. IGF-1 suppresses Bim expression in multiple myeloma via epigenetic and posttranslational mechanisms. Blood. 2010;115(12):2430–40.

27. Schmidt EK, Clavarino G, Ceppi M, Pierre P. SUnSET, a nonradioactive method to monitor protein synthesis. Nat Methods. 2009;6(4):275–7.

28. Alaterre E, Ovejero S, Herviou L, de Boussac H, Papadopoulos G, Kulis M, et al. Comprehensive characterization of the epigenetic landscape in Multiple Myeloma.

Theranostics. 2022;12(4):1715–29.

29. Le Floch R, Chiche J, Marchiq I, Naïken T, Ilk K, Murray CM, et al. CD147 subunit of lactate/H+ symporters MCT1 and hypoxia-inducible MCT4 is critical for energetics and growth of glycolytic tumors. Proc Natl Acad Sci U S A. 2011;108(40):16663–8.
30. Chang SH, Luo S, O'Brian KK, Thomas TS, Colditz GA, Carlsson NP, et al. Association between metformin use and progression of monoclonal gammopathy of undetermined signifi cance to multiple myeloma in US veterans with diabetes mellitus: A population-based retrospective cohort study. Lancet Haematol. 2015;2(1):e30–6.
31. Sevim Dalva-Aydemir, Richa Bajpai, Maylyn Martinez, Kehinde U.A. Adekola, Irawati Kandela, Changyong Wei, Seema Singhal, Jennifer E. Koblinski, Noopur S. Raje, Steven T. Rosen and MS. Targeting the Metabolic Plasticity of Multiple Myeloma with FDA- Approved Ritonavir and Metformin. Clin Cancer Res. 2015;21(5):1161–71.
32. Shanmugam M, McBrayer SK, Qian J, Raikoff K, Avram MJ, Singhal S, et al. Targeting glucose consumption and autophagy in myeloma with the novel nucleoside analogue 8-aminoadenosine. J Biol Chem. 2009;284(39):26816–30.
33. Evans LA, Anderson EA, Jessen E, Nandakumar B, Atilgan E, Jevremovic D, et al. Overexpression of the energy metabolism transcriptome within clonal plasma cells is associated with the pathogenesis and outcomes of patients with multiple myeloma. Am J Hematol. 2022;97(7):895–902.
34. Wang Y, Xu W, Yan Z, Zhao W, Mi J, Li J, et al. Metformin induces autophagy and G0/G1 phase cell cycle arrest in myeloma by targeting the AMPK/mTORC1 and mTORC2 pathways. J Exp Clin Cancer Res. 2018;37: 63.
35. Guo W, Kuang Y, Wu J, Wen D, Zhou A, Liao Y, et al. Hexokinase 2 Depletion Confers Sensitization to Metformin and Inhibits Glycolysis in Lung Squamous Cell Carcinoma. Front Oncol. 2020;10: 52.
36. de Smedt E, Devin J, Muylaert C, Robert N, Requirand G, Vlummens P, et al. G9a/GLP targeting in MM promotes autophagy-associated apoptosis and boosts proteasome inhibitor-mediated cell death. Blood Adv. 2021;5(9):2325–38.

37. Hideshima T, Nakamura N, Chauhan D, Anderson KC. Biologic sequelae of interleukin-6 induced PI3-K/Akt signaling in multiple myeloma. Oncogene. 2001;20(42):5991–6000.

Figures

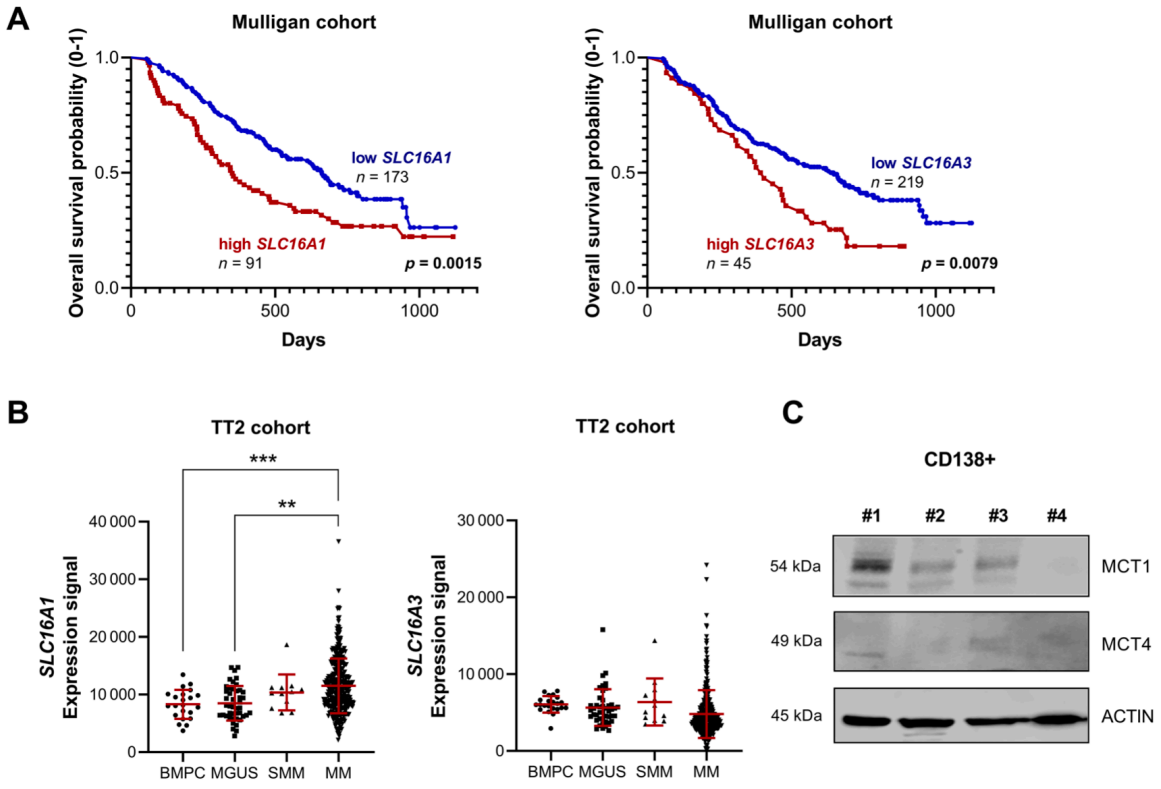

Figure 1. High MCT1 and MCT4 levels correlate with lower overall survival in MM patients. (A) Survival curves for MM patients with low (blue line) or high (red line) expression levels of *SLC16A1* (MCT1) (202236_s_at) or *SLC16A3* (MCT4) (202856_s_at) in the Mulligan cohort [23], analysed using GenomicScape. (B) *SLC16A1* (MCT1) and *SLC16A3* (MCT4) expression levels through different stages of MM development (BMPC n=22, MGUS n=44, SMM n=12, MM n=345) in the TT2 cohort [21,22]. Significance was determined by one-way ANOVA. (C) Protein expression levels of MCT1 and MCT4 in CD138+ MM cells from four different patients. Statistical significance was indicated as $p \leq 0.05$ (*), $p \leq 0.01$ (**) and $p \leq 0.001$ (***). MCT = monocarboxylate transporter, HR = hazard ratio, BMPC = bone marrow plasma cells, GUS = monoclonal gammopathy of undetermined significance, MM = multiple myeloma.

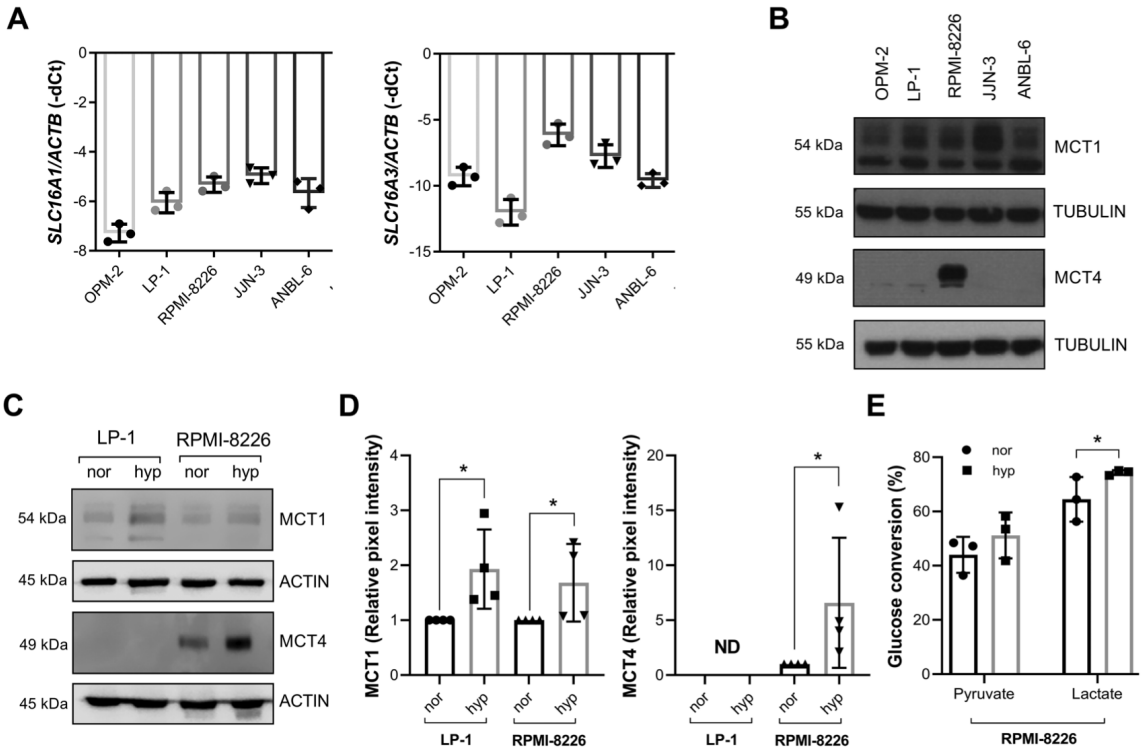

Figure 2. Lactate metabolism is upregulated in a hypoxic MM cells. (A) Basal RNA expression levels of *SLC16A1* (MCT1) and *SLC16A3* (MCT4) in five MM cell lines, measured by RT-qPCR in normoxic conditions (n=3). (B) Basal protein expression levels of MCT1 and MCT4 in five MM cell lines, measured by western blotting in normoxic conditions (n=3). (C,D) Protein expression levels of MCT1 and MCT4 measured by western blotting after 24 h of hypoxic culture (n=4). Pixel intensities for MCT1 and MC4 were normalized using the pixel intensity for β-Actin. (E) Tracer study measuring the glucose-to-pyruvate and glucose-to-lactate conversion by supplementing the RPMI-8226 cells with ^{13}C-glucose, comparing normoxia to hypoxia (n=3). Significance was determined using a Kruskal–Wallis test or Mann–Whitney U-test. Statistical significance was indicated as $p \leq 0.05$ (*). MCT = monocarboxylate transporter, nor : normoxia, hyp = hypoxia.

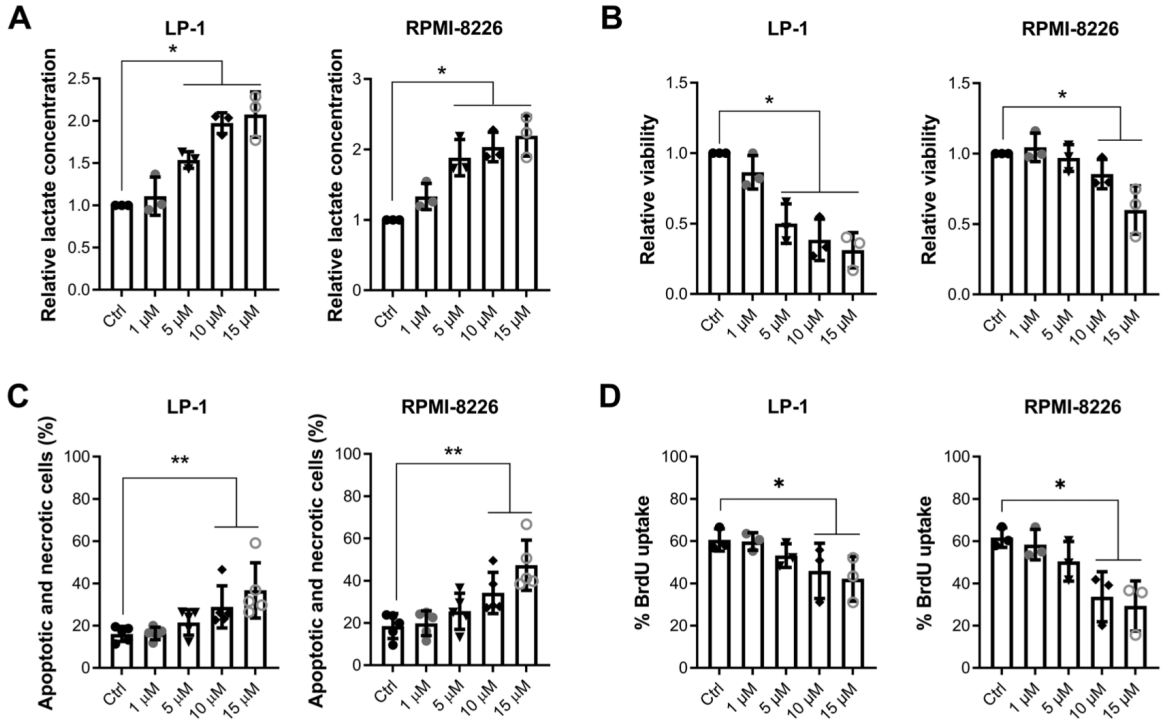

Figure 3. Syrosingopine reduces viability in MM by blocking lactate export. LP-1 and RPMI-8226 were treated with increasing doses (1–15 µM) of syrosingopine. (A) Intracellular lactate concentrations were measured after 3 h of hypoxic culture by LactateGlo (n=3). (B) Viability was measured after 48 h of hypoxic culture (n=3). (C) The percentage of apoptotic and necrotic cells was measured after 48 h of hypoxic culture by flow cytometry (n=5). (D) BrdU uptake was measured after 24 h of hypoxic culture by flow cytometry (n=3). Significance was determined using a Mann-Whitney U test. Statistical significance was indicated if $p \leq 0.05$ (*).

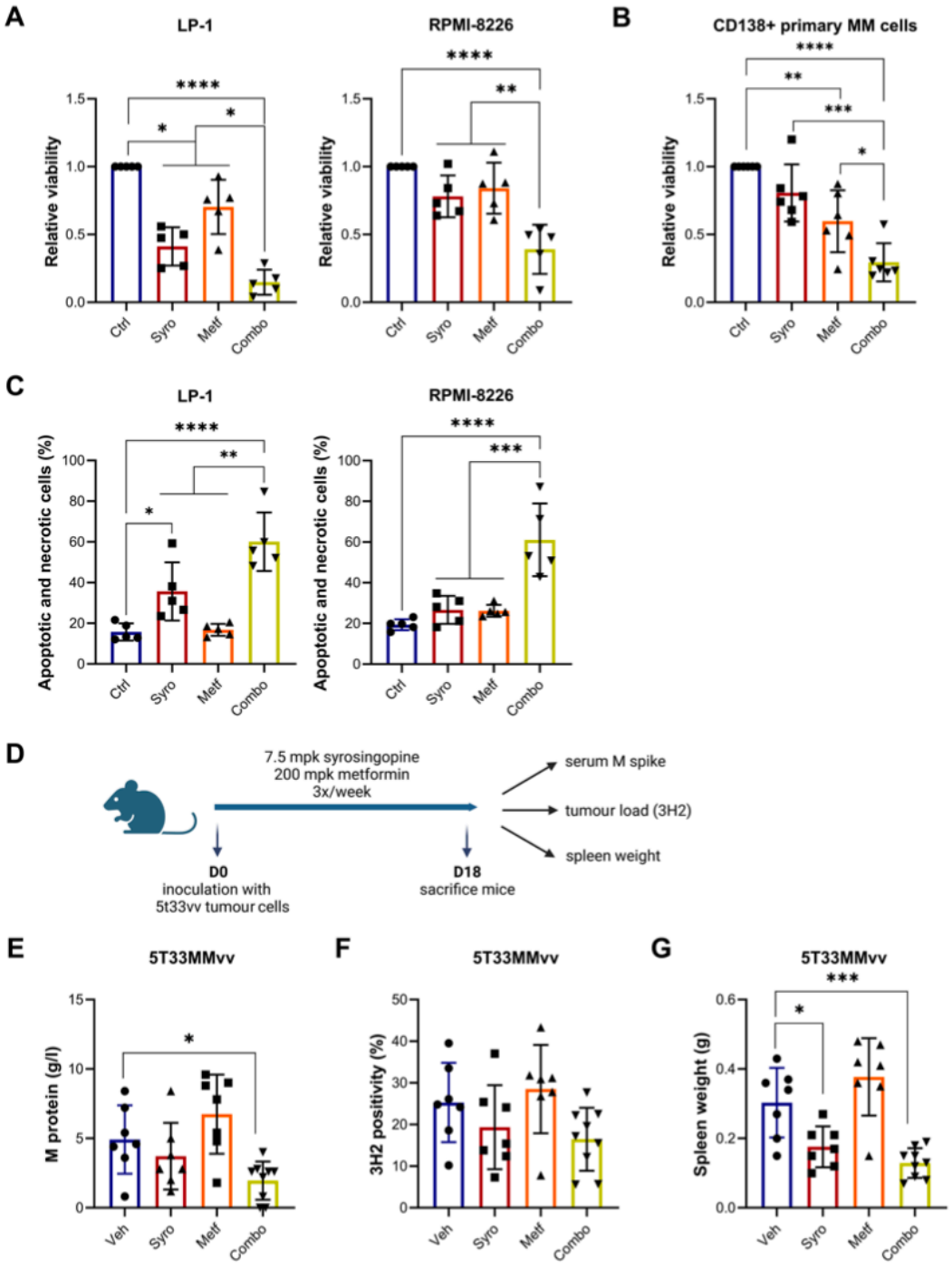

Figure 4. Metformin enhances sensitivity to syrosingopine *in vitro* and *in vivo*. (A) LP-1 and RPMI-8226 cells were treated with 10 µM syrosingopine and/or 10 mM metformin. Cells were cultured in hypoxia and viability was measured after 72 h (LP-1) or 48 h (RPMI-8226) using CellTiterGlo (n=5). (B) CD138+ cells derived from MM patients were treated with 10 µM syrosingopine and 10 mM metformin. Viability was measured after 24 h using CellTiterGlo (n=6). (C) LP-1 and RPMI-8226 cells were treated with 10 µM syrosingopine and 10 mM metformin.

Cells were cultured in hypoxia and apoptosis and necrosis was measured after 72 h (LP-1) or 48 h (RPMI-8226) by flow cytometry (n=5). (D-G) Schematic overview of experimental *in vivo* set-up. Syngeneic mice were injected with 0.5 million 5T33MMvv cells and treated with 7.5 mpk and/or 200 mpk metformin, 3 times a week. Mice were sacrificed on day 18 and tumour burden was analysed based on M-spike in blood serum, presence of idiotype (3H2) in BM derived cells, and spleen weight. Significance was determined by one-way ANOVA test. Statistical significance was indicated as $p \leq 0.05$ (*), $p \leq 0.01$ (**), $p \leq 0.001$ (***) and $p \leq 0.0001$ (****). Ctrl = control, Syro = syrosingopine, Metf = metformin, combo = combination of syrosingopine and metformin.

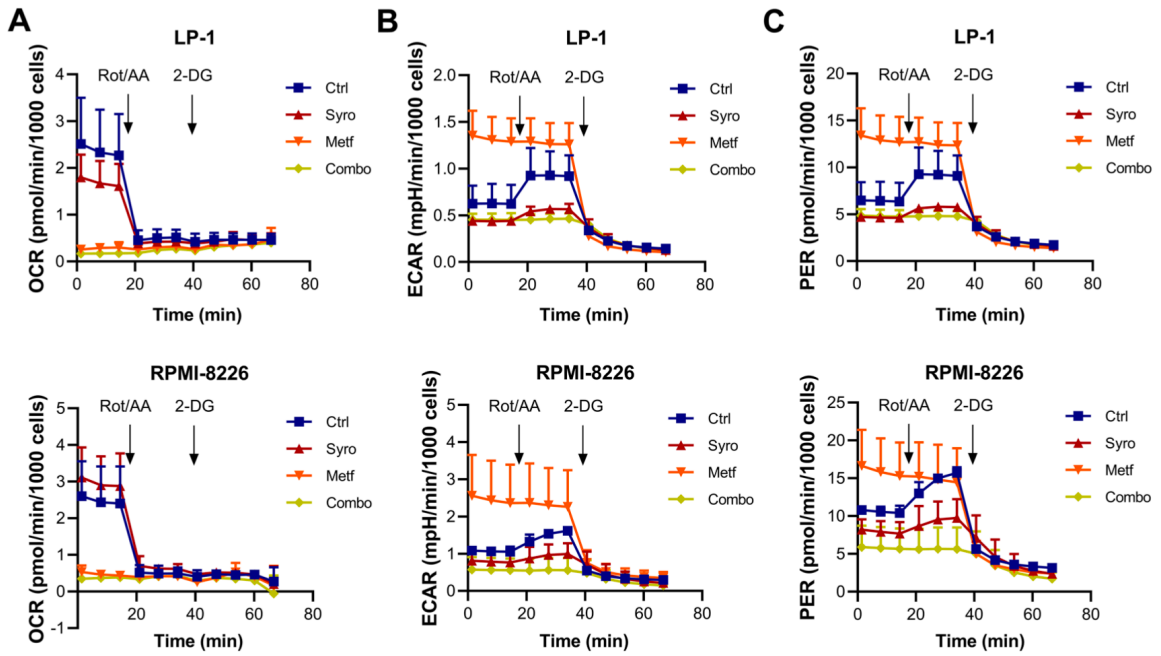

Figure 5. Syrosingopine and metformin induce changes in glycolytic and mitochondrial fluxes, respectively, in MM cell lines. (A,B) LP-1 and RPMI-8226 were treated with 10 µM of syrosingopine and/or 10 mM metformin for 16 h in hypoxia. Glycolytic and mitochondrial bioenergetics were measured and analysed using the Glycolytic Rate Assay through Agilent XFe Seahorse technology according to the manufacturer's instructions. Briefly, baseline oxygen consumption rates (OCR) and extracellular acidification rates (ECAR) were measured using the default protocol, consisting of three measurements in cycles of 5 min and automatic injection of Rotenone/Antimycin A (0.5 µM, after 18 min) and 2-deoxyglucose (50 mM, after 36 min) during a period of 70 min. The proton efflux rates (PER) are calculated based on the OCR and ECAR measurements. Results are shown as mean ± SD (n=3). Ctrl = control, Syro = syrosingopine, Metf = metformin, combo = combination of syrosingopine and metformin, Rot = rotenone, AA = antimycin A, 2-DG = 2-deoxyglucose, OCR = oxygen consumption rate, ECAR = extracellular acidification rate, PER = proton efflux rate

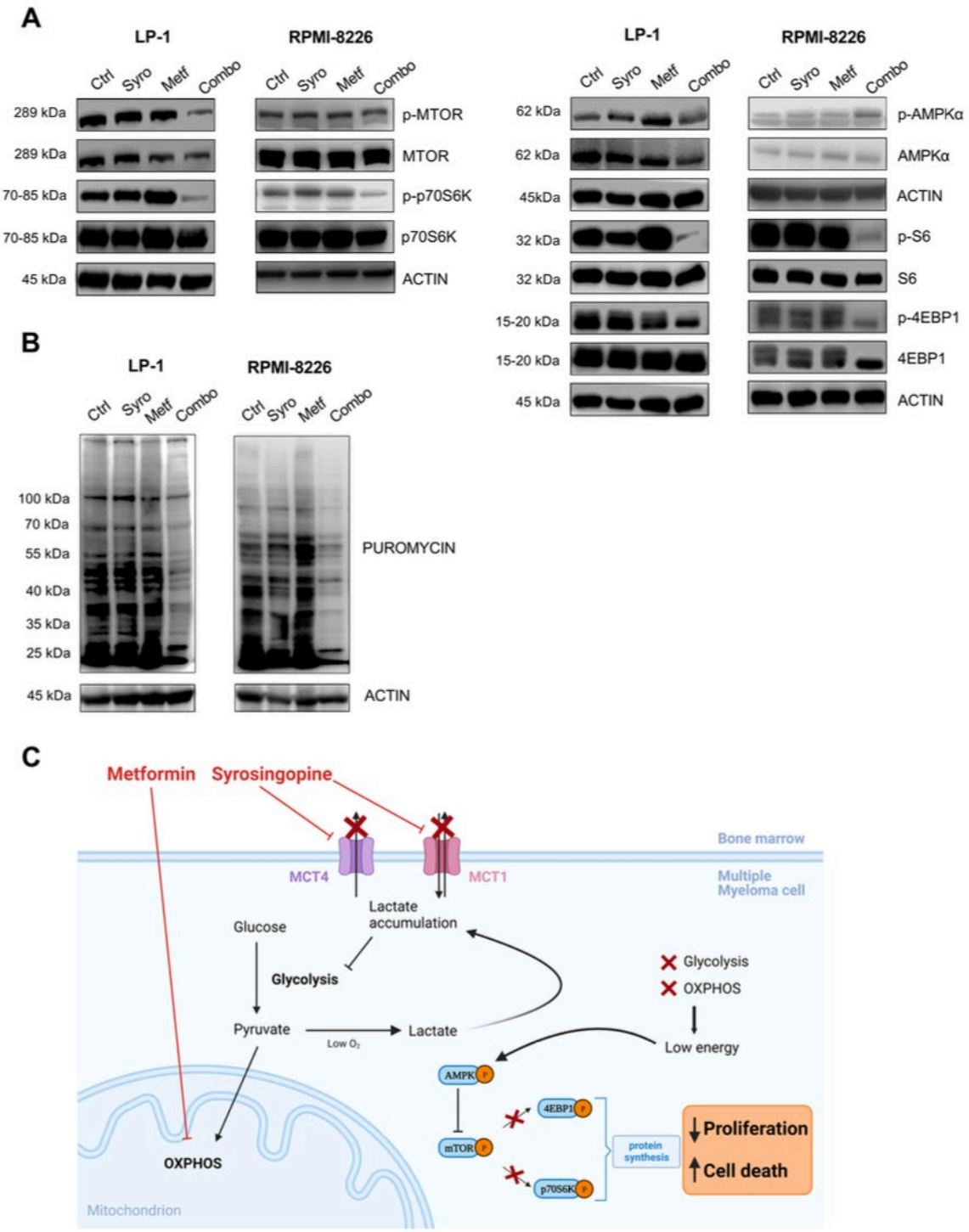

Figure 6. Metformin and syrosingopine reduce MM proliferation through a decrease in mTOR-mediated protein synthesis. (A) LP-1 and RPMI-8226 were treated with 10 µM of syrosingopine and 10 mM metformin and incubated for 16 h in hypoxic conditions. (A) Western blott analysis for proteins related to protein synthesis (n=5). (B) Western blot analysis of puromycin uptake (n=5). All experiments were performed in hypoxic conditions. (C) Graphical

abstract indicating intracellular effects of syrosingopine/metformin treatment. Created with Biorender.com. Ctrl = control, Syro = syrosingopine, Metf = metformin, combo = combination of syrosingopine and metformin

SUPPLEMENTARY MATERIAL ONLINE

Figure S1. CoMMpass study reveals *SLC16A1* and *SLC16A3* as genes linked to poor prognosis.

Figure S2. Dual inhibition of MCT1 and MCT4 synergizes with metformin in MM.

Figure S3. Quantification of pixel intensities for mTOR pathway analysis and puromycin uptake.